Journal of Power Sources 191 (2009) 209–216

Contents lists available at ScienceDirect

Journal of Power Sources

journal homepage: www.elsevier.com/locate/jpowsour

Hollow Ni–SiO_2 nanosphere-catalyzed hydrolytic dehydrogenation of ammonia borane for chemical hydrogen storage

Tetsuo Umegaki, Jun-Min Yan, Xin-Bo Zhang, Hiroshi Shioyama, Nobuhiro Kuriyama, Qiang Xu*

National Institute of Advanced Industrial Science and Technology (AIST), 1-8-31 Midorigaoka, Ikeda, Osaka, 563-8577, Japan

ARTICLE INFO

Article history:
Received 4 November 2008
Received in revised form 18 February 2009
Accepted 19 February 2009
Available online 4 March 2009

Keywords:
Nickel clusters
Hollow sphere
Hydrolysis
Ammonia borane
Hydrogen generation

ABSTRACT

Nickel clusters contained within silica nanospheres (20–30 nm) were synthesized by using a $Ni(NH_3)_6Cl_2$ crystal template method in a polyoxyethylene–nonylphenyl ether/cyclohexane reversed micelle system followed by an in situ reduction in aqueous $NaBH_4/NH_3BH_3$ solutions. Metallic nickel clusters exist inside the SiO_2 nanospheres prepared by the method while oxidized nickel clusters prepared by the conventional impregnation method were supported on the outer surface of silica as shown in the results of transmission electron microscope (TEM)/energy dispersive X-ray (EDX) and X-ray photoelectron spectroscopy (XPS) measurements. The nickel clusters inside of silica nanospheres show higher catalytic activity for hydrolysis of ammonia borane to generate stoichiometric amount of hydrogen than the supported nickel catalysts.

1. Introduction

Hydrogen is a globally accepted clean fuel. The use of hydrogen fuel cells in portable electronic devices or vehicles requires lightweight hydrogen storage or on-board hydrogen generation. Although there have been a large number of reports on hydrogen storage materials [1,2] and on on-board reforming of hydrocarbon into hydrogen [3], big challenges still remain. For hydrogen storage materials, the gravimetric and volumetric hydrogen capacities must be improved, whereas for the on-board reforming, the difficulty in operating the system at high temperature poses an obstacle to its practical application. Chemical hydrides, due to their high hydrogen contents, are expected as potential hydrogen sources for PEM fuel cells. Among them, boron- and nitrogen-based compounds such as $LiNH_2$–LiH and $NaBH_4$ have attracted much attention [4–6]. Ammonia borane, NH_3BH_3, which has a hydrogen capacity of 19.6 wt.%, exceeding that of gasoline, have made itself an attractive candidate for chemical hydrogen storage applications. Intensive efforts have been made to enhance the kinetics of the hydrogen release from this compound from both solid and solution approaches [7–19].

A high-performance hydrogen generation system based on transition metal-catalyzed dissociation and hydrolysis of ammonia borane, NH_3BH_3, at room temperature has been achieved [8–16]. NH_3BH_3 dissolves in water to form a solution stable in the absence of air. The addition of a catalytic amount of suitable metal catalysts into the solutions leads to rapid release of hydrogen gas with an H_2 to NH_3BH_3 ratio up to 3.0. Not only noble metal but also non-noble metal-based catalysts exhibit high activities to this reaction [8,10–16]. This hydrogen generation system possesses high potential to find its application to portable fuel cells. For practical use, low-cost and high-performance non-noble metal catalysts are desired. Studies of catalysts for hydrogen generation from aqueous ammonia borane solution show that dispersion of active metals and/or amorphousness of active phase play important roles in the catalytic performances [10–13,15,16].

Nanoparticles coating with spherical silica or within silica hollow sphere have been attracting more and more interests due to their great potential applications in the areas of photonics [20–24], magnetics [25], catalysis [26–30,32], and absorbents [31–33]. The preparation of nanoparticles in a reverse micelle system has attracted great attention because of its possibility to obtain monodispersed particles in nanometer size [21,24–33]. In addition, the water pool in the reverse micelle cage can be expected as hydrolysis and polymerization reaction field of the silica. For example, metal clusters in hollow SiO_2 nanospheres were successfully synthesized by using crystal template method with metal ammine complexes into NP-6/cyclohexane reversed micelle system [31–33].

The present paper reports that hollow Ni–SiO_2 nanospheres exhibit high catalytic activity for hydrogen generation from hydrolysis of ammonia borane.

* Corresponding author. Tel.: +81 72 751 9562; fax: +81 72 751 9629.
E-mail address: q.xu@aist.go.jp (Q. Xu).

0378-7753/$ – see front matter © 2009 Elsevier B.V. All rights reserved.
doi:10.1016/j.jpowsour.2009.02.054

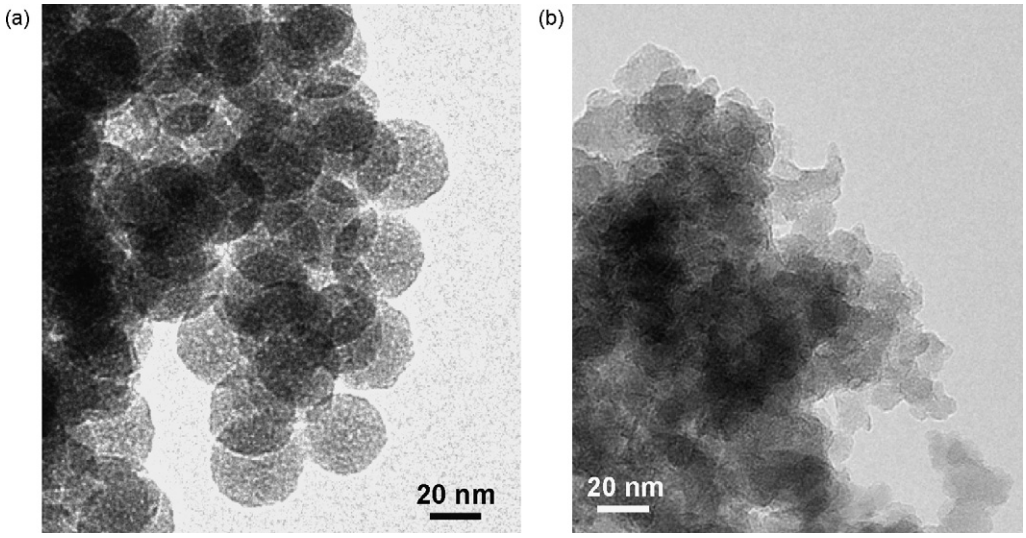

Fig. 1. TEM images of (a) hollow Ni–SiO_2 nanospheres and (b) commercial SiO_2 supported Ni catalyst before hydrolysis of NH_3BH_3.

2. Experimental

2.1. Catalyst preparation

Hollow Ni–SiO_2 nanospheres were prepared by reversed micelle techniques as follows. Aqueous hexaamminenickel chloride ($Ni(NH_3)_6Cl_2$, Mitsuwa Chem. Co., >99.0%) solution (3.6 mL) was rapidly injected into 800 mL of NOIGEN EA-80 (polyoxyethylene–nonylphenyl ether; supplied by Daiichi Kogyo Seiyaku Co.) cyclohexane (Kishida Chem. Co., >99.5%) solution. The concentrations of $Ni(NH_3)_6Cl_2$ were 80, 160, and 400 mM, which determined the Ni contents of the products $Ni/(Ni + SiO_2) = 4.3$, 8.3, and 18.5 wt.%, respectively. After stirring at room temperature for 12 h, 3.6 mL of 28 wt.% aqueous ammonia solution (Kishida Chem. Co.) was injected rapidly and after 2 h, 1.39 mL of tetraethoxysilane ($Si(OC_2H_5)_4$, Kishida Chem. Co., >99.0%) were added rapidly. The solution was transparent at the beginning but slightly cloudy after 2 days stirring. The resulting solution was phase separated by the addition of methyl alcohol (Kishida Chem. Co., 99.8%), followed by filtration and washing with cyclohexane and acetone (Kishida Chem. Co., >99.5%). After drying in a desiccator overnight, the obtained light blue fine powders were used as catalysts.

SiO_2 supported Ni catalysts used in this study were prepared by the conventional impregnation method. Commercial SiO_2 (specific surface area = 380 $m^2\,g^{-1}$, Aldrich, 99.8%) and SiO_2 nanospheres prepared similarly to the preparation of hollow Ni–SiO_2 nanospheres were used as the catalytic support. For preparing SiO_2 supported catalysts, impregnation was performed by evaporating SiO_2 support with aqueous $Ni(NH_3)_6Cl_2$ solution at 303 K.

2.2. Characterization

The morphologies of the hollow Ni–SiO_2 nanospheres and the SiO_2 supported Ni catalysts were observed using a Tecnai G^2 20 Twin transmission electron microscope (TEM) operating with an acceleration voltage of 200 kV, which was equipped with CCD camera (Gatan Image Filter) and an energy dispersive X-ray (EDX) detector.

Powder X-ray diffraction (XRD) was performed on a RINT-2200 X-ray diffractometer with a Cu Kα source (40 kV, 40 mA) for the hollow Ni–SiO_2 nanospheres and the SiO_2 supported Ni catalysts. The catalysts were held on a glass substrate and covered by an adhesive tape on the surface to minimization the samples exposure to oxygen and moisture during the measurement.

X-ray photoelectron spectra were acquired with an ESCA-3400 spectrometer (Shimadzu Corp.) equipped with a Mg Kα X-ray exciting source (1253.6 eV) operating at 10 kV and 10 mA. The binding energies (BE) were referred to the C 1s peak at 285.0 eV. After the initial data were collected, a 2 kV Ar^+ sputter beam was used for depth profiling of the samples before and after hydrolysis of NH_3BH_3.

2.3. Experimental procedures for hydrolysis of ammonia borane

A mixture of sodium borohydride ($NaBH_4$, 10 mg, Aldrich, >98.5%), ammonia borane (NH_3BH_3, 55 mg, Aldrich, 90%), and catalyst was kept in a two-necked round-bottom flask. One neck was connected to a gas burette, and the other was connected to a pressure-equalization funnel to introduce distilled water (10 mL). The reaction started when distilled water was introduced to the mixture of $NaBH_4$, NH_3BH_3, and the catalyst, and the evolution of gas was monitored using the gas burette. The reactions were carried out at room temperature in argon. Additionally, the molar ratio of catalyst to reactant (Ni/NH_3BH_3) was changed with various values (0.01, 0.02, 0.05) for catalytic reactions in argon.

All the samples after hydrolysis of NH_3BH_3 were centrifugally separated from the reaction solution, and then dried in desiccator under vacuum condition.

3. Results and discussion

The morphologies of hollow Ni–SiO_2 nanospheres and commercial SiO_2 supported Ni catalysts before hydrolysis of NH_3BH_3 were examined using TEM. The TEM image of the hollow Ni–SiO_2 nanospheres reveals that the sample consists of spherical particles with 20–30 nm diameter (Fig. 1a), while the TEM image of the commercial SiO_2 supported Ni catalyst reveals that the sample consists of amorphous phase (Fig. 1b). Both the samples give the TEM images of low contrast, with which we cannot identified Ni particles. To confirm the presence of Ni by agglomeration of Ni clusters, we have carried out TEM and EDX spectrometry experiments of the hollow Ni–SiO_2 nanospheres and the commercial SiO_2 supported Ni catalyst before hydrolysis of NH_3BH_3 with heat treatment in H_2

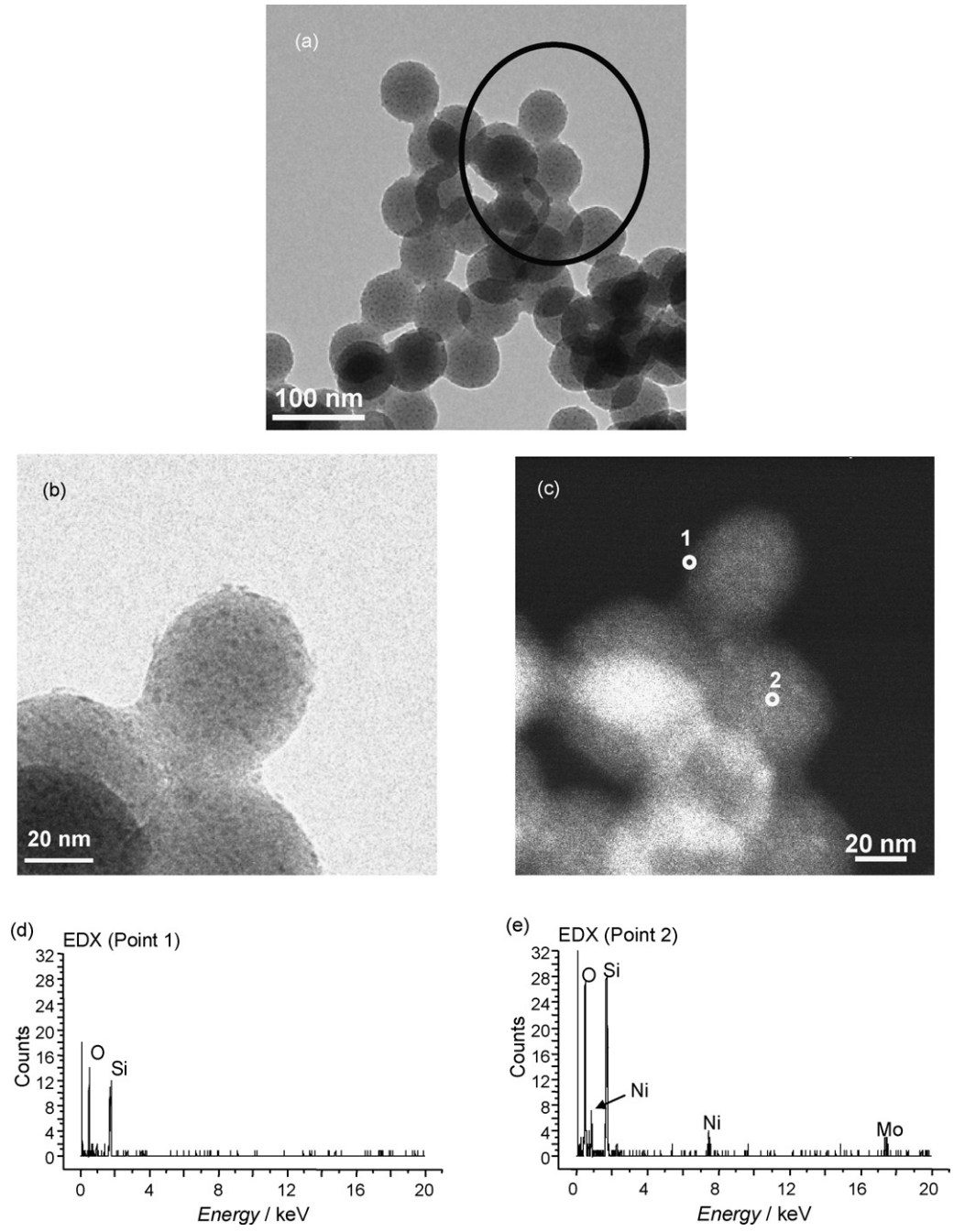

Fig. 2. TEM images (a and b) and HAADF image (c) of the H_2-treated hollow Ni–SiO_2 nanospheres, and the corresponding EDX spectra (d and e).

flow at 773 K for 5 h after evacuation procedure at 573 K for 5 h. Fig. 2 shows the TEM images (a and b) and the high angle annular dark field (HAADF) image (c) of the H_2-treated hollow Ni–SiO_2 nanospheres, and the corresponding EDX spectra (d and e). Many spherical substances with diameters of 20–30 nm including darker spots with diameters of <ca. 3 nm can be found in Fig. 2a and b. The EDX spectrum (Fig. 2d) for point 1 marked in Fig. 2c exhibits Kα peaks corresponding to O (0.51 keV) and Si (1.74 keV) elements, whereas another EDX spectrum (Fig. 2e) for point 2 marked in Fig. 2c exhibits Kα peaks corresponding to O, Ni (0.86 and 7.49 keV), and Si elements. The Mo signal at 17.48 keV in Fig. 2e is from the TEM grid. The spectra indicate that Ni particles with diameters of <ca. 3 nm were located inside a spherical SiO_2 nanoparticle. Whereas, the TEM image (Fig. 3a) of the H_2-treated commercial SiO_2 supported Ni catalyst reveals that darker spots with diameter of <ca. 100 nm can be observed on the outer surface of amorphous substances. The EDX spectrum (Fig. 3c) for point 1 marked in Fig. 3b exhibits Kα peaks corresponding to O and Si elements, whereas another EDX spectrum (Fig. 3d and e) for point 2 and 3 marked in Fig. 3b exhibits Kα peaks corresponding to O, Ni, and Si elements. The spectra indicate that Ni particles with diameters of <ca. 100 nm were located on the SiO_2 surface for the commercial SiO_2 supported Ni catalyst.

Fig. 4 shows time course of the hydrogen evolution from aqueous NH_3BH_3 solution in the presence of hollow Ni–SiO_2 nanospheres, SiO_2 nanospheres supported Ni catalyst, and commercial SiO_2 supported Ni catalyst. The reaction rate and the amount of hydrogen evolution significantly depend on the catalysts. The evolution of

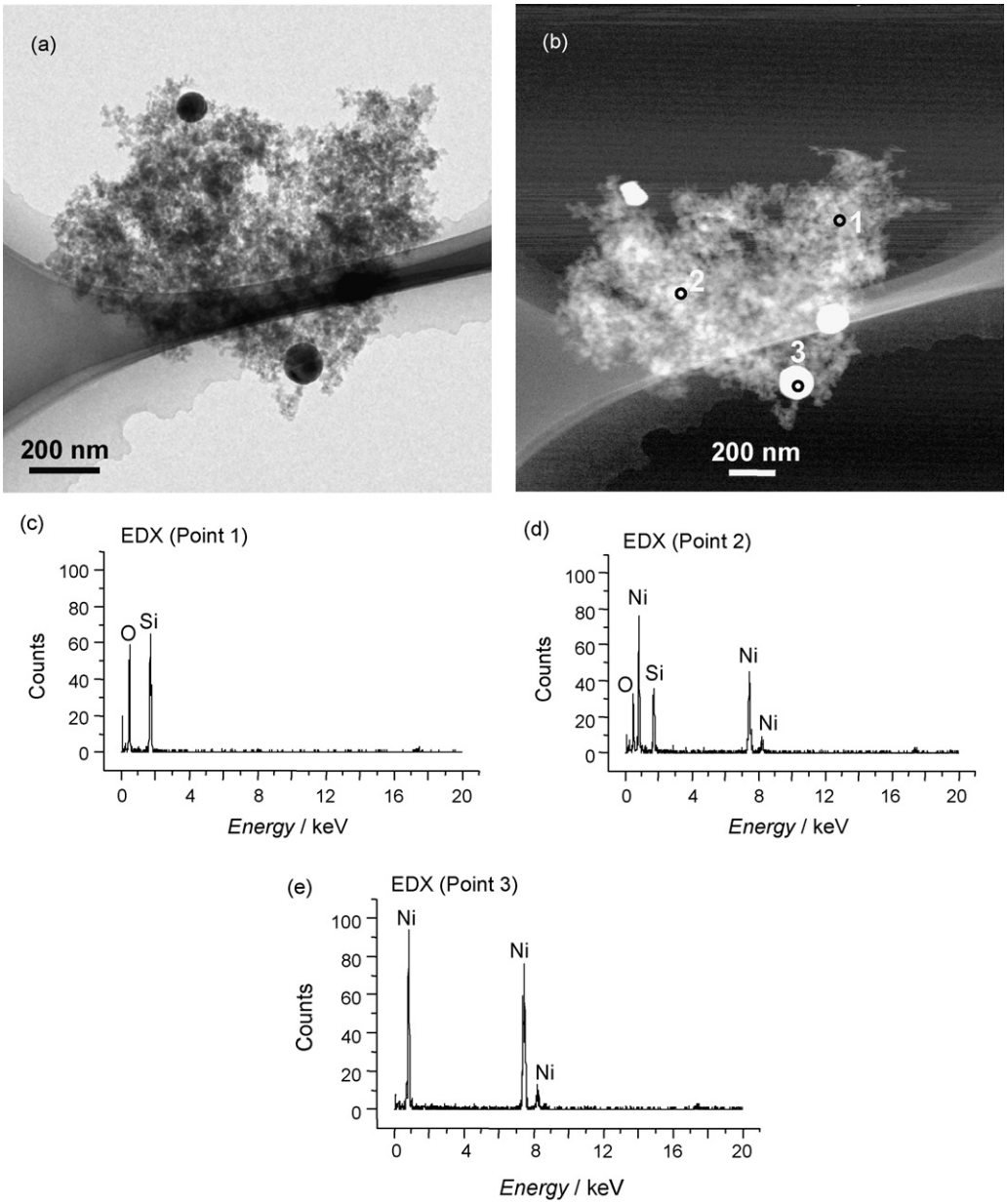

Fig. 3. TEM image (a) and HAADF image (b) of the H_2-treated commercial SiO_2 supported Ni catalyst, and the corresponding EDX spectra (c–e).

139, 102, and 96 mL hydrogen were finished in 22, 76, and 120 min in the presence of hollow Ni–SiO_2 nanospheres, SiO_2 nanospheres supported Ni catalyst, and commercial SiO_2 supported Ni catalyst, respectively. As shown in the inset of Fig. 4, only negligible amount of hydrogen is generated without adding of $NaBH_4$ in the presence of hollow Ni–SiO_2 nanospheres and NH_3BH_3. The result suggests that $NaBH_4$ is necessary to activate the catalysts. The effect of $NaBH_4$ has been reported about Fe catalyst for hydrolysis of NH_3BH_3 [12]. In the present reaction system, $NaBH_4$ was mixed with H_2O, NH_3BH_3, and catalyst. Hydrogen is evolved via following two reactions:

$$NaBH_4 + 2H_2O \rightarrow Na^+ + BO_2^- + 4H_2 \quad (1)$$

$$NH_3BH_3 + 2H_2O \rightarrow NH_4^+ + BO_2^- + 3H_2 \quad (2)$$

In the present reaction condition, about 20 mL hydrogen is generated via reaction (1), and about 120 mL hydrogen is generated via reaction (2). The molar ratio of hydrolytically generated hydrogen to the initial NH_3BH_3 in the presence of hollow Ni–SiO_2 nanospheres, SiO_2 nanospheres supported Ni catalyst, and commercial SiO_2 supported Ni catalyst are 3.0, 2.0, and 1.9, respectively. The theoretical molar ratio of the reaction completion is 3.0, thus the results indicate that dehydrogenation is completed in the presence of hollow Ni–SiO_2 nanospheres, while in the presence of the SiO_2 supported Ni catalysts the dehydrogenation is not completed or there may be side reactions which cause less hydrogen release. For making clear the reason of the released H_2 to NH_3BH_3 ratio less than 3.0, we further added aqueous NH_3BH_3 solution into the solution after the hydrolysis of $NaBH_4$ and NH_3BH_3 mixture in the presence of the commercial SiO_2 supported Ni catalyst and observed further release of 2.2 equiv. of hydrogen, indicating that the commercial SiO_2 supported Ni catalyst keeps its catalytic activity during the reaction. To check if there is unreacted NH_3BH_3 in the resulting solution, we added highly active PtO_2 [8] into the resulting solution and observed no hydrogen release. The dependence of equilibrium com-

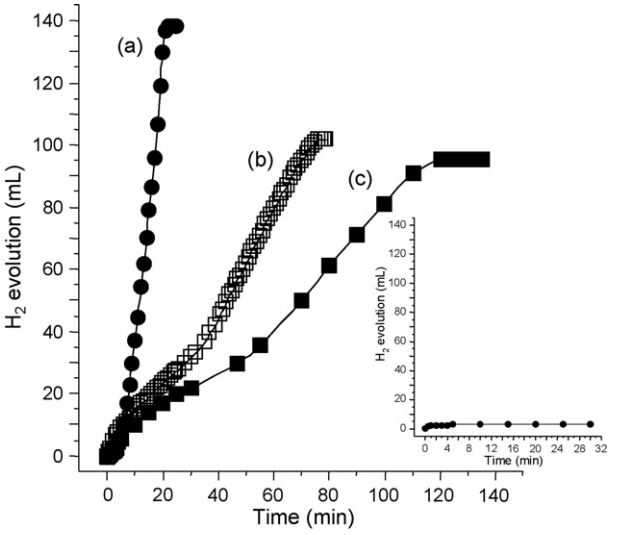

Fig. 4. Hydrogen generation from hydrolysis of ammonia borane (0.16 M, 10 mL) with $NaBH_4$ in the presence of (a) hollow Ni–SiO_2 nanospheres, (b) SiO_2 nanospheres supported Ni catalyst, (c) commercial SiO_2 supported Ni catalyst, and without $NaBH_4$ in the presence of hollow Ni–SiO_2 nanospheres (inset). Ni/NH_3BH_3 = 0.05 (in argon atmosphere).

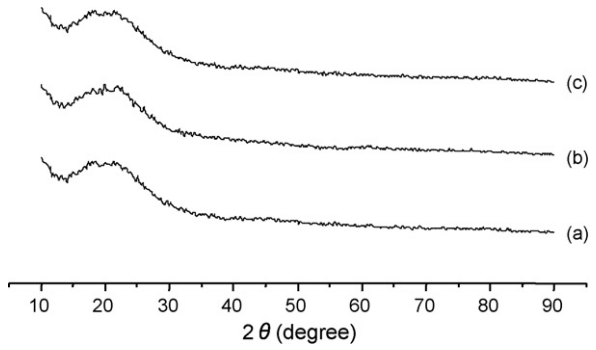

Fig. 5. Powder X-ray diffraction patterns for (a) the hollow Ni–SiO_2 nanospheres, (b) the SiO_2 nanospheres supported Ni catalyst, and (c) the commercial SiO_2 supported Ni catalyst after hydrolysis of NH_3BH_3.

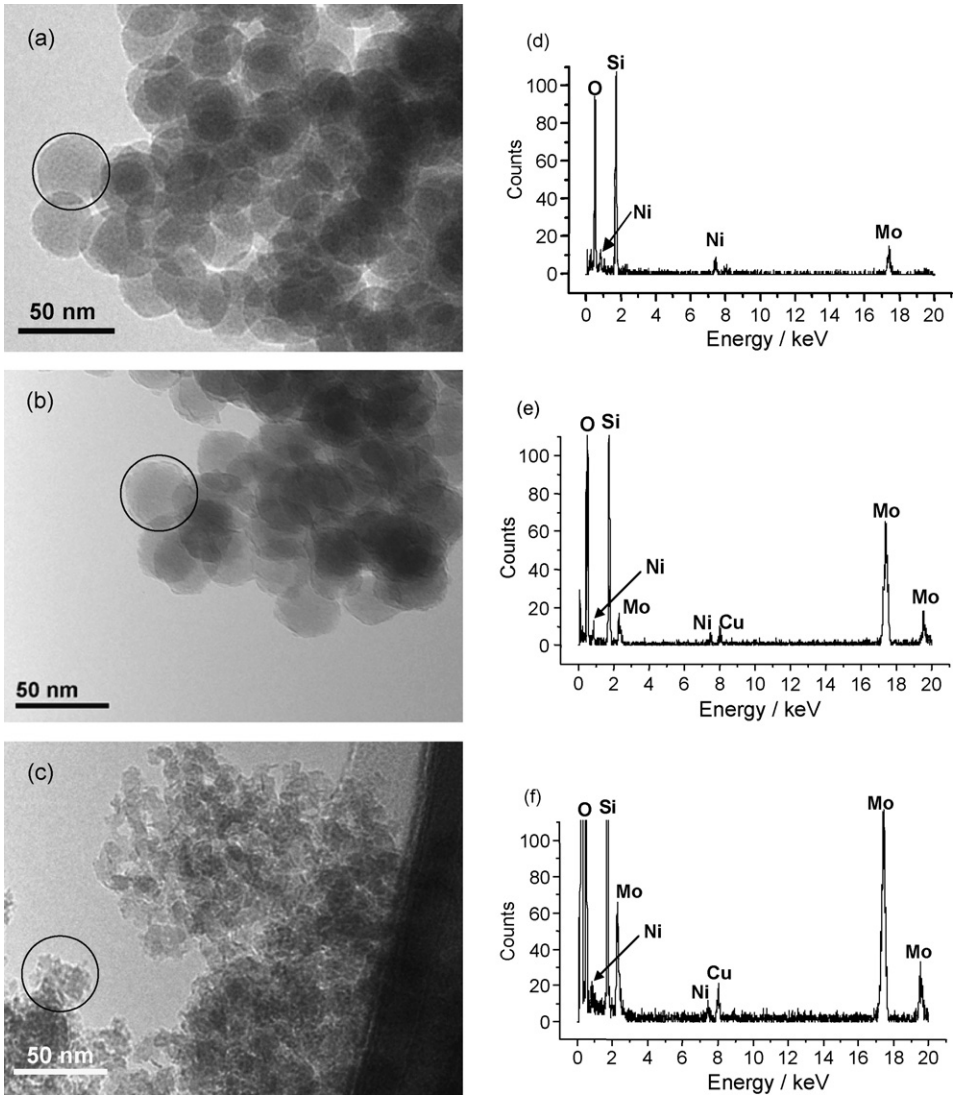

Fig. 6. TEM images of (a) the hollow Ni–SiO_2 nanospheres, (b) the SiO_2 nanospheres supported Ni catalyst, and (c) the commercial SiO_2 supported Ni catalyst after hydrolysis of NH_3BH_3, and the corresponding EDX spectra (d–f).

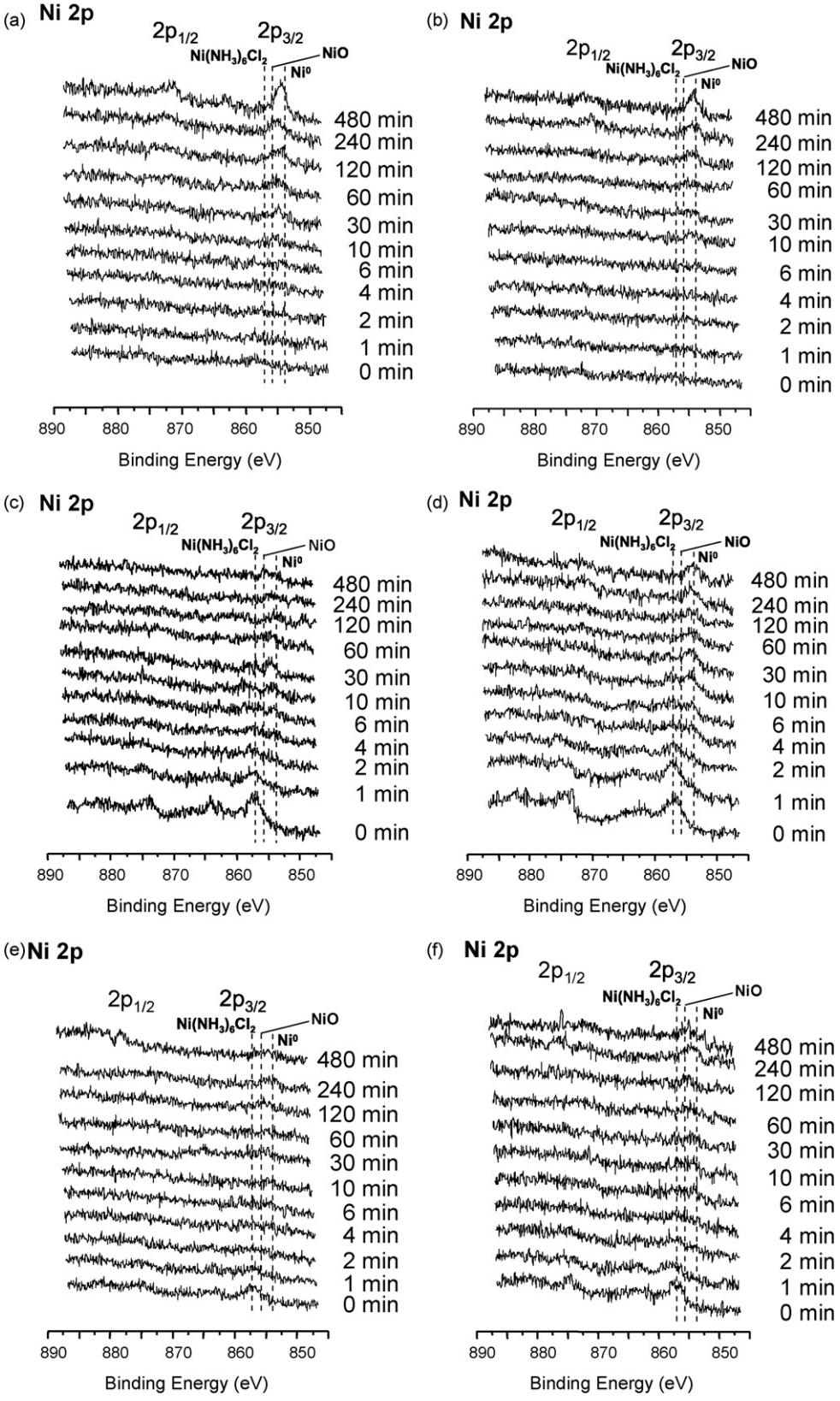

Fig. 7. Ni 2p XPS spectra obtained from the hollow Ni–SiO_2 nanospheres before and after hydrolysis of NH_3BH_3 (a and b), SiO_2 nanospheres supported Ni catalysts before and after hydrolysis of NH_3BH_3 (c and d), and commercial SiO_2 supported Ni catalysts before and after hydrolysis of NH_3BH_3 (e and f). The profiles were obtained using 2 keV-Ar^+ sputtering times of 0, 1, 2, 4, 6, 10, 30, 60, 120, 240, and 480 min.

positions on the catalysts is because of possible side reaction along with hydrolysis of NH_3BH_3, such as dehydrogenation of NH_3BH_3 as follows [17–19]:

$$NH_3BH_3 \rightarrow H_2NBH_2 + H_2 \quad (3)$$

$$H_2NBH_2 \rightarrow HNBH + H_2 \quad (4)$$

Less amount of hydrogen (1 or 2 equiv. of hydrogen) is generated via the reactions than via hydrolysis of NH_3BH_3 (3 equiv. of hydrogen). It has been observed that less amount of hydrogen than stoichiometric amount of hydrogen from hydrolysis of NH_3BH_3 is generated according to catalysts, for example, in the presence of Pd black [8], Pt-, and Ni-based alloys [13,14], and Cu-based catalysts [16].

We analyzed the X-ray diffraction patterns of hollow Ni–SiO_2 nanospheres and SiO_2 supported Ni catalysts after hydrolysis of NH_3BH_3. All the XRD profiles for the hollow Ni–SiO_2 nanospheres and the SiO_2 supported Ni catalysts show no diffraction line assignable to any nickel species (Fig. 5). The results indicate Ni particles in all the catalysts are amorphous after hydrolysis of NH_3BH_3.

The morphologies of hollow Ni–SiO_2 nanospheres, SiO_2 nanospheres supported Ni catalyst, and SiO_2 supported Ni catalysts after hydrolysis of NH_3BH_3 were examined using TEM and energy dispersive X-ray (EDX) spectrometry. The TEM images of the hollow Ni–SiO_2 nanospheres and the SiO_2 nanospheres supported Ni catalyst reveals that both the samples consist of spherical nanoparticles with 20–30 nm diameters (Fig. 6a and b), while the TEM image of the commercial SiO_2 supported Ni catalyst reveals that the sample consists of amorphous phase (Fig. 6c). All the samples give the TEM images of low contrast, with which we cannot identified Ni particles. To confirm the presence of Ni, we have carried out EDX experiments. Fig. 6d–f shows the EDX spectra of the region marked in Fig. 6a–c. The EDX spectra exhibits Kα peaks corresponding to O, Ni, and Si elements, Mo signals (2.33, 17.48, and 19.54 keV) from the TEM grid, and Cu signals (8.04 keV) from the sample holder for TEM grid. The EDX analysis indicates a particle in the hollow Ni–SiO_2 nanospheres and the SiO_2 supported Ni catalysts includes Ni.

We analyzed the X-ray photoelectron spectroscopy (XPS) of the hollow Ni–SiO_2 nanospheres before and after hydrolysis of NH_3BH_3 in combination with argon ion etching to confirm the presence of Ni inside of the SiO_2 nanospheres. Fig. 7a and b shows the Ni 2p spectra of the hollow Ni–SiO_2 nanospheres before and after hydrolysis of NH_3BH_3, respectively. In order to obtain the depth profiles, the samples were sputtered with 2 keV-Ar^+ for 0, 1, 2, 4, 6, 10, 30, 60, 120, 240, and 480 min. The Ni $2p_{3/2}$ and/or Ni $2p_{1/2}$ peaks of both the samples can be observed after 10 min of sputtering from Fig. 7a and b. The Si 2p and O 1s peaks of the hollow Ni–SiO_2 nanospheres before and after hydrolysis of NH_3BH_3 are observed all the sputtering times, thus the result suggests Ni clusters exist inside the SiO_2 nanoparticles. The spectra of the hollow Ni–SiO_2 nanospheres before and after hydrolysis of NH_3BH_3 exhibits a Ni $2p_{3/2}$ band at 854.6–855.2 eV and at 854.3–854.6 eV shown in Fig. 7a and b. Whereas, the spectra of the metal nickel, NiO, and $Ni(NH_3)_6Cl_2$ exhibit Ni $2p_{3/2}$ band at 853.7, 855.7, and 857 eV, respectively. These results indicate that some part of Ni metal clusters in the hollow Ni–SiO_2 nanospheres before and after hydrolysis of NH_3BH_3 were partially oxidized, suggesting that many Ni atoms on the surface of the metal clusters interacted directly with Si–O–Ni bond, in agreement with the results obtained by the XANES/EXAFS measurements [30], and slightly larger number of metallic Ni exists in the hollow Ni–SiO_2 nanospheres after hydrolysis of NH_3BH_3 than that in the hollow Ni–SiO_2 nanospheres before hydrolysis of NH_3BH_3 as the report about the reduction degree of nickel on SiO_2 support [34]. Otherwise, the spectra of the SiO_2 nanospheres supported Ni catalyst before and after hydrolysis of NH_3BH_3 exhibit Ni $2p_{3/2}$ band at 857.2 and 857.0 eV, and Ni $2p_{1/2}$ band at 874.2 and 874.4 eV before Ar^+ sputtering, respectively (Fig. 7c and d), which are typical of Ni^{2+} ions [34]. With increasing sputtering time, both peaks decrease and almost disappear after 4 min. The Ni $2p_{3/2}$ peak appears again after 120 and 30 min sputtering. The spectra exhibit Ni $2p_{3/2}$ band around 854.5 eV, which is due to partially oxidized Ni atoms. These results suggest that the completely oxidized Ni clusters exist on the outer surface of SiO_2 and the partially oxidized Ni clusters exist in the pore of SiO_2, and Ni clusters are partially dispersed into the inside of SiO_2 nanospheres during hydrolysis reaction. The spectra of commercial SiO_2 supported Ni catalysts before and after hydrolysis of NH_3BH_3 exhibit Ni $2p_{3/2}$ band at 857.2 and 857.3 eV, and Ni $2p_{1/2}$ band at 875.4 and 874.7 eV before Ar^+ sputtering (Fig. 7e and f), which are typical of Ni^{2+} ions [34]. With increasing sputtering time, all the peaks decrease and almost disappear after 2 min. The Ni $2p_{3/2}$ peaks of the commercial SiO_2 supported Ni catalyst before and after hydrolysis of NH_3BH_3 appear again after 240 min sputtering. Both the spectra exhibit Ni $2p_{3/2}$ bands around 855 eV, which is due to partially oxidized Ni atoms. These results suggest that the completely oxidized Ni clusters exist on the outer surface of SiO_2 and the partially oxidized Ni clusters exist in the pore of SiO_2, and the difference of the peak positions between the profiles before and after hydrolysis of NH_3BH_3 is small, indicating that the Ni oxidation states in the supported catalysts are similar before and after hydrolysis of NH_3BH_3. The results show that the more metallic Ni corresponds to higher catalytic activity for hydrolysis of NH_3BH_3. In the present reaction system, oxidized Ni is first reduced by $NaBH_4$ to metallic Ni, which catalyzes the hydrolysis of NH_3BH_3.

The hydrogen evolution from hydrolysis of aqueous NH_3BH_3 solution in the presence of the hollow Ni–SiO_2 nanospheres with different Ni loadings shows in Fig. 8. The evolution of 139, 136, and 136 mL hydrogen was finished in 22, 24 and 25 min in the presence of the samples with $Ni/(Ni + SiO_2) = 4.3$, 8.3 and 18.5 wt.%, respectively. The molar ratio of hydrolytically generated hydrogen to the initial NH_3BH_3 is 3.0 in the presence of each catalyst, indicating all the samples with different Ni loadings show high catalytic activity for hydrolysis of NH_3BH_3 to generate stoichiometric amount of hydrogen.

Fig. 9 shows the hydrogen evolution from hydrolysis of aqueous NH_3BH_3 solution with various Ni/NH_3BH_3 molar ratios. The

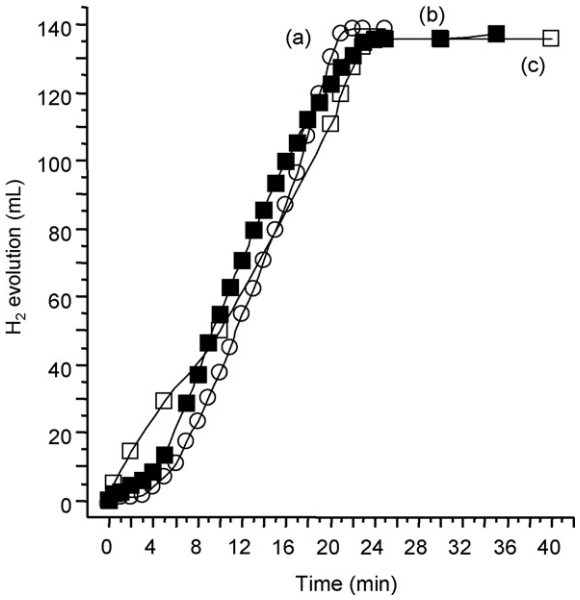

Fig. 8. The effect of Ni loading on hydrogen generation from hydrolysis of ammonia borane (0.16 M, 10 mL) in the presence of hollow Ni–SiO_2 nanospheres. $Ni/(Ni + SiO_2)$ = (a) 4.3 wt.%, (b) 8.3 wt.%, and (c) 18.5 wt.%.

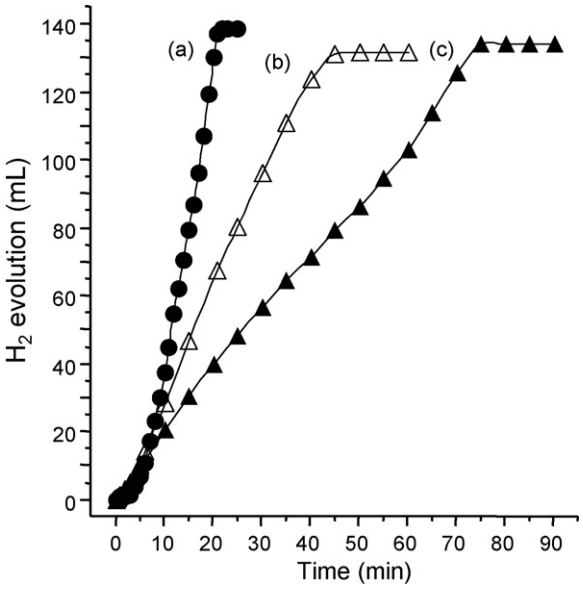

Fig. 9. Hydrogen evolution for the hydrolysis of ammonia borane (0.16 M, 10 mL) in the presence of hollow Ni–SiO_2 nanospheres with various molar ratio of Ni/NH_3BH_3 in argon. Ni/NH_3BH_3 = (a) 0.5, (b) 0.2, and (c) 0.1.

evolution of 134, 132, and 139 mL hydrogen was finished in approximately 75, 45, 22 min for Ni/NH_3BH_3 molar ratios of 0.01, 0.02, and 0.05, respectively. The molar ratios of hydrolytically generated hydrogen to the initial NH_3BH_3 are 3.0, 2.9, and 3.0 for Ni/NH_3BH_3 of 0.01, 0.02, and 0.05, respectively. The results indicate the reaction completed time decreases with increase of Ni/NH_3BH_3 molar ratios.

4. Conclusion

Nickel clusters contained within silica nanospheres (20–30 nm) were synthesized by using a $Ni(NH_3)_6Cl_2$ crystal template method in a polyoxyethylene–nonylphenyl ether/cyclohexane reversed micelle system followed by an in situ reduction in aqueous $NaBH_4/NH_3BH_3$ solutions, whereas nickel clusters prepared by conventional impregnation method were supported on the outer surface of silica. The morphologies of the hollow Ni–SiO_2 nanospheres and the SiO_2 supported Ni catalyst are identified by TEM/EDX measurements. The hollow Ni–SiO_2 nanospheres show higher catalytic activity for hydrolysis of ammonia borane to generate stoichiometric amount of hydrogen than the SiO_2 supported Ni catalysts. The results of XPS depth profiles suggest that the metallic Ni clusters exist inside the SiO_2 nanoparticles of hollow Ni–SiO_2 nanospheres, whereas for the SiO_2 supported Ni catalyst the oxidized Ni clusters exist on the outer surface of SiO_2 and partially oxidized Ni clusters exist in the pore of SiO_2.

Acknowledgements

The authors would like to thank NEDO and AIST for financial support and Dr. Akita and Mr. Uchida for TEM measurements.

References

[1] L. Schlapbach, A. Züttel, Nature 414 (2001) 353–358.
[2] N.L. Rosi, J. Eckert, M. Eddaoudi, D.T. Vodak, J. Kim, M. O'Keeffe, O.M. Yaghi, Science 300 (2003) 1127–1129.
[3] G.A. Deluga, J.R. Salge, L.D. Schmidt, X.E. Verykios, Science 303 (2004) 993–997.
[4] P. Chen, Z. Xiong, J. Luo, J. Lin, K.L. Tan, Nature 420 (2002) 302–304.
[5] S.C. Amendola, S.L. Sharp-Goldman, M. Saleem Janjua, M.T. Kelly, P.J. Petillo, M. Binder, J. Power Sources 85 (2000) 186–189.
[6] S.C. Amendola, S.L. Sharp-Goldman, M. Saleem Janjua, N.C. Spencer, M.T. Kelly, P.J. Petillo, M. Binder, Int. J. Hydrogen Energy 25 (2000) 969–975.
[7] A. Gutowska, L. Li, Y. Shin, C.M. Wang, X.S. Li, J.C. Linehan, R.S. Smith, B.D. Kay, B. Schmid, W. Shaw, M. Gutowski, T. Autrey, Angew. Chem. Int. Ed. 44 (2005) 3578–3582.
[8] M. Chandra, Q. Xu, J. Power Sources 156 (2006) 190–194.
[9] M. Chandra, Q. Xu, J. Power Sources 159 (2006) 855–860.
[10] Q. Xu, M. Chandra, J. Power Sources 163 (2006) 364–370.
[11] M. Chandra, Q. Xu, J. Power Sources 168 (2007) 135–142.
[12] J.-M. Yan, X.-B. Zhang, S. Han, H. Shioyama, Q. Xu, Angew. Chem. Int. Ed. 47 (2008) 2287–2289.
[13] F. Cheng, H. Ma, Y. Li, J. Chen, Inorg. Chem. 46 (2007) 788–794.
[14] C.F. Yao, L. Zhuang, Y.L. Cao, X.P. Ai, H.X. Yang, Int. J. Hydrogen Energy 33 (2008) 2462–2467.
[15] S.B. Kalidindi, M. Indirani, B.R. Jagirdar, Inorg. Chem. 47 (2008) 7424–7429.
[16] S.B. Kalidindi, U. Sanyal, B.R. Jagirdar, Phys. Chem. Chem. Phys. 10 (2008) 5870–5874.
[17] R.J. Keaton, J.M. Blacquiere, R. Tom Baker, J. Am. Chem. Soc. 129 (2007) 1844–1845.
[18] F.H. Stephens, V. Pons, R. Tom Baker, Dalton Trans. (2007) 2613–2626.
[19] M.C. Denney, V. Pons, T.J. Hebden, D. Michael Heinekey, K.I. Goldberg, J. Am. Chem. Soc. 128 (2006) 12048–12049.
[20] M. Giersig, T. Ung, L.M. Liz-Marzán, P. Mulvaney, Adv. Mater. 9 (1997) 570–575.
[21] W. Wang, S.A. Asher, J. Am. Chem. Soc. 123 (2001) 12528–12535.
[22] T. Torimoto, J. Paz Reyes, K. Iwasaki, B. Pal, T. Shibayama, K. Sugawara, H. Takahashi, B. Ohtani, J. Am. Chem. Soc. 125 (2003) 316–317.
[23] Y. Yang, M. Gao, Adv. Mater. 17 (2005) 2354–2357.
[24] Y. Yang, L. Jing, X. Yu, D. Yan, M. Gao, Chem. Mater. 19 (2007) 4123–4128.
[25] T. Haeiwa, K. Segawa, K. Konishi, J. Magn. Magn. Mater. 310 (2007) e809–e811.
[26] T. Miyao, N. Toyoizumi, S. Okuda, Y. Imai, K. Tajima, S. Naito, Chem. Lett. (1999) 1125–1126.
[27] A.J. Zarur, J.Y. Ying, Nature 403 (2000) 65–67.
[28] M. Ikeda, T. Tago, M. Kishida, K. Wakabayashi, Chem. Commun. (2001) 2512–2513.
[29] S. Takenaka, K. Hori, H. Matsune, M. Kishida, Chem. Lett. 34 (2005) 1594–1595.
[30] S. Takenaka, H. Umebayashi, E. Tanabe, H. Matsune, M. Kishida, J. Catal. 245 (2007) 392–400.
[31] T. Miyao, K. Minoshima, S. Naito, J. Mater. Chem. 15 (2005) 2268–2270.
[32] S. Naito, K. Minoshima, T. Miyao, Top. Catal. 39 (2006) 131–136.
[33] T. Miyao, K. Minoshima, Y. Kurokawa, K. Shinohara, W. Shen, S. Naito, Catal. Today 132 (2008) 132–137.
[34] K. Hadjiivanov, M. Mihaylow, D. Klissurski, P. Stefanov, N. Abadjieva, E. Vassileva, L. Mintchev, J. Catal. 185 (1999) 314–323.